

Evaluating the reliability of using the deflection amplification factor to estimate design displacements with accidental torsion effects

Jui-Liang Lin^{*1}, Wei-Chun Wang^{2a} and Keh-Chyuan Tsai^{2b}

¹National Center for Research on Earthquake Engineering, Taiwan

²Department of Civil Engineering, National Taiwan University, Taiwan

(Received July 13, 2014, Revised November 5, 2014, Accepted December 23, 2014)

Abstract. Some model building codes stipulate that the design displacement of a building can be computed using the elastic static analysis results multiplied by the deflection amplification factor, C_d . This approach for estimating the design displacement is essential and appealing in structural engineering practice when nonlinear response history analysis (NRHA) is not required. Furthermore, building codes stipulate the consideration of accidental torsion effects using accidental eccentricity, whether the buildings are symmetric-plan, or asymmetric-plan. In some model building codes, the accidental eccentricity is further amplified by the torsional amplification factor A_x in order to minimize the discrepancy between statically and dynamically estimated responses. Therefore, this warrants exploration of the reliability of statically estimated design displacements in accordance with the building code requirements. This study uses the discrepancy curves as a way of assessing the reliability of the design displacement estimates resulting from the factors C_d and A_x . The discrepancy curves show the exceedance probabilities of the differences between the statically estimated design displacements and NRHA results. The discrepancy curves of 3-story, 9-story, and 20-story example buildings are investigated in this study. The example buildings are steel special moment frames with frequency ratios equal to 0.7, 1.0, 1.3, and 1.6, as well as existing eccentricity ratios ranging from 0% to 30%.

Keywords: reliability; deflection amplification factor; accidental torsion effect; torsional amplification factor; seismic responses; nonlinear response history analysis

1. Introduction

It is widely accepted that inelastic dynamic analysis, also designated nonlinear response history analysis (NRHA), is the most reliable approach for assessing structural seismic responses when compared with inelastic static analysis and elastic static analysis. The accuracy of seismic response estimates of multistory buildings obtained from inelastic static analysis, i.e., the pushover analysis, was comprehensively investigated (Krawinkler and Seneviratna 1998, Kim and D'Amore 1999,

*Corresponding author, Research Fellow, E-mail: jlilin@ncree.narl.org.tw

^aGraduate Student, E-mail: r00521203@ntu.edu.tw

^bProfessor, E-mail: kctsai@ntu.edu.tw

Gupta and Kunnath 2000, Krawinkler *et al.* 2011). These research results provide useful insights into the reliability of using inelastic static analysis to estimate the seismic responses of real buildings. Nevertheless, the reliability of using elastic static analysis to estimate the seismic responses of multistory buildings remains unclear. In this study, elastic static analysis means that the deflection at level x (δ_x) used to compute the design story drift is estimated using the elastic static analysis results multiplied by the deflection amplification factor C_d (ASCE/SEI 7-10 2010)

$$\delta_x = \frac{C_d \delta_{xe}}{I_e} \quad (1)$$

where δ_{xe} is the deflection at level x determined by elastic static analysis, and I_e is the importance factor assigned to the building. The relevant C_d values for some common building systems stipulated in Table 12.2-1 of ASCE/SEI 7-10 are summarized in Table 1.

Similarly, Eurocode 8 (2004) stipulates that if linear analysis is performed, the displacements induced by the design seismic ground motion, denoted as d_s , shall be calculated on the basis of the elastic deformations, d_e , of the structural system as

$$d_s = q_d d_e \quad (2)$$

where q_d is the displacement behavior factor, assumed to be equal to the behavior factor, q , unless otherwise specified. The values of factor q for some common building systems (from Tables 5.1 and 6.2 of Eurocode 8) are shown in Table 2. The approximate values of α_u/α_1 , shown in Table 2 for various building systems, are provided in Eurocode 8. For example, the suggested value of α_u/α_1 is 1.3 for multistory multi-bay steel moment-resisting frames. When the aforementioned building frames are not regular in plan, the value of α_u/α_1 is further modified as the average of one and 1.3, i.e., 1.15. Thus, for steel moment-resisting frame systems with regular elevation and high ductility, the values of the displacement behavior factor q_d are 6.5 (i.e., 5×1.3) and 5.75 (i.e., 5×1.15) for regular-plan and irregular-plan systems, respectively. It is interesting to compare these two values, i.e., 6.5 and 5.75, with the corresponding C_d value, which is equal to 5.5 for steel special moment frames, as stipulated in ASCE/SEI 7-10 (Table 1). In this comparison, the deflection estimate provided by ASCE/SEI 7-10 is less than the estimate provided by Eurocode 8. Therefore, Eurocode 8 is a little conservative compared to ASCE/SEI 7-10 in this case.

It is worth noting that C_d and q_d are not equal to the inelastic deformation ratio defined as ratio of the peak deformation of an inelastic system to that of the corresponding elastic system. Figure 1 shows the force–deformation relationship of a structural system. According to the symbols used in Fig. 1, the aforementioned inelastic deformation ratio is equal to u_m/u_0 , hereby denoted as C . Moreover, C_d/I_e and q_d are equal to u_m/u_e . Thus, it is clear that the relationship between factor C_d/I_e and factor C is

$$\frac{C_d}{I_e} = \frac{u_m}{u_e} = \frac{u_m}{u_0} \frac{u_0}{u_y} \frac{u_y}{u_e} = CR_y \alpha_1 \quad (3)$$

where $R_y = u_0/u_y$ is the yield strength reduction factor; and α_1 , equal to u_y/u_e , is further discussed in the Note section of Table 2. The abovementioned elastic static approaches (Eqs. 1 and 2) for estimating the deflections of multistory buildings stipulated in model building codes ASCE/SEI 7-

10 and Eurocode 8 are critical and appealing in structural engineering practice. Typically, studies of the inelastic deformation ratio, C , were carried out using single-degree-of-freedom systems (Veletsos and Newmark 1960, Iwan 1980, Fajfar 2000, Miranda 2000, Miranda and Ruiz-Garcia 2002, Chopra and Chintanapakdee 2004, Ruiz-Garcia and Miranda 2006). Therefore, this warrants a direct investigation into the reliability of deflection estimates for multistory buildings obtained using the code-specified elastic static approach.

Table 1 Deflection amplification factors, C_d , for some common building systems, as stipulated in ASCE/SEI 7-10

Seismic Force-Resisting System	C_d
Special reinforced concrete shear walls	5
Special reinforced concrete moment frames	5.5
Steel special moment frames	5.5
Steel eccentrically braced frames	4
Steel special concentrically braced frames	5
Steel buckling-restrained braced frames	5
Steel special plate shear walls	6

Table 2 Behavior factors^a, q , for some common building systems, as stipulated in Eurocode 8

Structural Type		Ductility Class	
		DCM	DCH
Concrete Bldg.	Frame system, dual system, coupled wall system	$3.0\alpha_u/\alpha_1$	$4.5\alpha_u/\alpha_1$
	Uncoupled wall system	3	$4.0\alpha_u/\alpha_1$
	Torsionally flexible system	2	3
Steel Bldg.	Moment-resisting frames	4	$5\alpha_u/\alpha_1$
	Moment-resisting frame with concentric bracing	4	$4\alpha_u/\alpha_1$
	Frame with eccentric bracings	4	$5\alpha_u/\alpha_1$

Note:

^a If the building is non-regular in elevation, then the listed values of behavior factor q should be reduced by 20%. In addition, for concrete buildings, the listed values of behavior factor q should be modified by multiplying the factor k_w , reflecting the prevailing failure mode in structural systems with walls. The value of factor k_w is equal to one for frame and frame-equivalent dual systems, and is equal to $0.5 \leq (1 + \alpha_0)/3 \leq 1$ for wall, wall-equivalent, and torsionally flexible systems, where α_0 is the prevailing aspect ratio of the walls of the structural system.

DCM: medium ductility

DCH: high ductility

α_1 is the value by which the horizontal seismic design action is multiplied in order to first reach the flexural resistance in any member in the structure, while all other design actions remain constant.

α_u is the value by which the horizontal seismic design action is multiplied in order to form plastic hinges in a number of sections sufficient for the development of overall structural instability, while all other design actions remain constant.

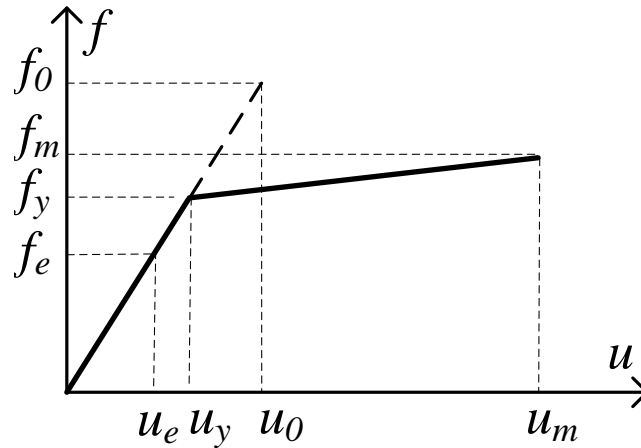


Fig. 1 Schematic drawing of the force–deformation relationship of a structural system

The inclusion of accidental torsion effects in the seismic design of buildings are mandated by model building codes whether the buildings are symmetric-plan or asymmetric-plan (De la Llera and Chopra 1994, Dimova and Alashki 2003). Both ASCE/SEI 7-10 and Eurocode 8 account for accidental torsion effects by requiring the center of mass (CM) of every story to be shifted by a distance of $\pm 5\% \times L_i$ away from its nominal position, where L_i is the floor plane dimension perpendicular to the direction of the applied ground motion. The plus and minus sign preceding the ‘5%’ indicate that consideration should be given to the shifted CM in either direction. When applying the static analysis approach, the model building code ASCE/SEI 7-10 (but not Eurocode 8) further amplified the accidental eccentricity, i.e., $\pm 5\% \times L_i$, by multiplying by the torsional amplification factor A_x . The factor A_x is defined as

$$1 \leq A_x = \left(\frac{\eta}{1.2}\right)^2 = \left(\frac{\delta_{\max}}{1.2\delta_{\text{avg}}}\right)^2 \leq 3 \quad (4)$$

where δ_{\max} is the maximum displacement at the x -th story, and δ_{avg} is the average of the displacements on both sides of the floor plane at the x -th story. Thus, it requires two stages of static analysis work to include the accidental torsion effects when analyzing in accordance with ASCE/SEI 7-10. The first stage is to shift the CM from the nominal position to a distance of $\pm 5\%$ of the floor plane and then perform the static analysis based on this modified building structure, from which the A_x value for every story is computed. The second stage of the analysis involves statically analyzing the twice-modified building with the CM of each story shifted from the nominal position to a distance of $\pm 5\% \times A_x$ of the floor plane. From this, the static analysis results are produced.

De la Llera and Chopra (1995) showed that there are general discrepancies between the seismic responses with accidental torsion effects found by using the static and dynamic analysis approaches. Thus, they developed static design procedures to achieve the design force increase due to accidental torsion in order to be consistent with that of the dynamic analysis approach. Furthermore, Dimova and Alashki (2003) pointed out that even for symmetric buildings with the 5% accidental eccentricity ratio, the static analysis procedures stipulated by Eurocode 8 may

underestimate the accidental torsional effects by up to 21%. Humar and Kumar (2000) studied the torsional provisions in some building codes by investigating a simple single-story model building with three resisting elements in one direction. They showed that the torsional provisions in UBC (1997) and the other four codes were conservative for element design on the flexible side of the building. Nevertheless, when the building has a low torsional stiffness value, the code provisions may not be conservative for element design on the stiff side of the building (Humar and Kumar 2000). Recently, DeBock *et al.* (2013) suggested that accidental torsion provisions in the ASCE/SEC 7-10 standard are not necessary for seismic design of buildings without excessive torsional flexibility or asymmetry because the provisions have a minor change in their collapse capacity. These aforementioned research results as a whole clearly indicate that the code-specified static analysis approach cannot completely reflect the accidental torsion effects on buildings when compared with the dynamically estimated responses. In order to understand the reliability of the statically estimated elastic seismic responses with accidental torsion effects, Wang *et al.* (2014) performed a related reliability assessment. The exceedance probabilities of the discrepancy between the statically and dynamically estimated elastic responses with accidental torsion effects for various multistory buildings were investigated. One of their conclusions was that there is a 65% chance for the statically estimated elastic displacement at the CM of a torsionally stiff 20-story building to be overestimated with a discrepancy higher than 40% (Wang *et al.* 2014).

Following the above discussion of code-specified elastic static analysis approaches and the existing research related to factors C_d and A_x , it clearly warrants investigation of the reliability of using the C_d factor specified by ASCE/SEI 7-10 to estimate the design displacements involving the effect of the A_x factor. Note that the torsional amplification factor A_x is stipulated clearly for the elastic static analysis. However, it is not so clear when the elastic response spectrum or history analysis method is considered. Therefore, even though the two aforementioned elastic dynamic analysis methods better consider the higher mode effects and reflects the dynamics of torsional properties, this study does not perform the reliability assessment of the design displacements predicted by using the elastic dynamic analysis methods. Based on the previously developed methodology (Wang *et al.* 2014), the stated reliability is presented in terms of the probability of exceedance for some discrepancy states. Discrepancy is defined as the difference between the design displacements estimated by using NRHA and conducting code-specified elastic static analysis.

2. Reliability assessment methodology

The reliability assessment methodology used in this study is based on previous research (Wang *et al.* 2014). Accordingly, this study also employs the discrepancy curves, which show the exceedance probability of discrepancy between statically and dynamically estimated responses, as a function of a certain structural parameter such as existing eccentricity. As part of a comprehensive study, the methodology for constructing discrepancy curves is discussed in the following.

2.1 Discrepancy curves

A discrepancy curve is the plot of a discrepancy function. The discrepancy function, $F_{dc'}(e)$, for the discrepancy state dc' (an absolute value of DC') is defined as

$$F_{dc'}(e) \equiv P[|DC'| \geq dc' | e] = \Phi \left(\frac{\ln \left(\frac{e}{\lambda} \right)}{\beta} \right) \quad (5a)$$

where the random variable DC' is the normalized difference between statically and dynamically estimated engineering demand parameters (EDP)

$$DC' = \frac{(EDP_{\pm 0.05 A_x})_{static} - (EDP_{\pm 0.05})_{dynamic}}{(EDP_{\pm 0.05})_{dynamic}} \times 100 \% \quad (5b)$$

In Eq. (5a), Φ denotes the standard normal (Gaussian) cumulative distribution function; λ denotes the medium value of the distribution; β denotes the logarithmic standard deviation; and e denotes the existing eccentricity ratio, which is the existing eccentricity divided by the floor plane dimension in the same direction. The existing eccentricity is the original distance between the CM and the center of rigidity (CR), excluding the accidental eccentricity. The $EDPs$ considered in this study include the peak displacement at the CM, the peak displacements on the flexible side (FS), and the stiff side (SS). The FS and SS are the two sides of a floor plane close to the CM and the CR, respectively. The subscripts 'static' and 'dynamic' (Eq. (5b)) indicate that the values in the associated parentheses result from the static analysis approach as specified in ASCE/SEI 7-10 (Eq. (1)), and the NRHA approach, respectively. The subscripts ' $\pm 0.05 A_x$ ' and ' ± 0.05 ' (Eq. (5b)) represent the ratios of the shifted distance of the CM to the floor plane dimension in the same direction. Equation (5b) indicates that only the accidental eccentricity used in the static analysis approach is further amplified from multiplying by the factor A_x , whereas the accidental eccentricity used in the dynamic analysis approach is not amplified. Since the random variable DC' (Eq. (5b)) may be positive or negative, the absolute value of the random variable DC' , denoted as $|DC'|$, is used in Eq. (5a). The discrepancy state dc' represents the extent of the discrepancy values. Table 3 defines four discrepancy states representing minor, moderate, severe, and unacceptable levels for the random variable $|DC'|$. The thresholds (Table 3) assumed to define the discrepancy states are generally subjective. For instance, the discrepancy value $|DC'|$ no greater than 10% has been arbitrarily considered as minor in this study. Certainly, based on a different tolerance required for specific purposes, 5% or 2% rather than 10% for example may be selected as the $|DC'|$ value to represent the minor discrepancy state. The consideration for selecting the four thresholds presented in this study is to avoid these discrepancy curves so close to each other that no significant differences could be observed among these curves.

2.2. Procedures for constructing discrepancy curves

The procedures for constructing the discrepancy curves of a group of buildings subjected to the

Table 3 $|DC'|$ values for defining the discrepancy states

Discrepancy State	$dc'1$ (minor)	$dc'2$ (moderate)	$dc'3$ (severe)	$dc'4$ (unacceptable)
$ DC' $ (%)	10	20	40	60

excitation of an ensemble of ground motions are stated below. The buildings in the group are identical except their existing eccentricity ratios range from 0% to 30% in 1% increments. In this study, considering an accidental eccentricity ratio of 5% represents a greater CM shift away from the CR. For an accidental eccentricity ratio of -5%, the CM is located closer to the CR. The procedures are performed once for each of the two cases. For brevity, ± 0.05 is used in the procedures instead of individually specifying an accidental eccentricity ratio of +5% or -5%. The procedures for constructing the discrepancy curves are stated as follows.

Step 1: NE and NM denote the total number of eccentricity ratios and ground motions considered, respectively. Set $i=1$ and $j=1$ to denote the number of eccentricity ratios and ground motions currently under consideration, respectively. Obviously, $1 \leq i \leq NE$ and $1 \leq j \leq NM$.

Step 2: Perform NRHA on the modified building, whereby the eccentricity ratio has changed to equal the sum of the existing eccentricity ratio, $e=(i-1) \times 0.01$, and the accidental eccentricity ratio, ± 0.05 , under the excitation of the j -th ground motion. The peak values of $EDPs$, denoted as $(EDP_{\pm 0.05})_{dynamic}$, for all floors are obtained from this analysis.

Step 3: Perform the elastic static analysis of the modified building. The seismic base shear, V , used in this static analysis is

$$V = \frac{S_a I_e}{R} W \quad (6)$$

The factor S_a is the design spectral acceleration. The factors R and I_e represent the response modification factor and the importance factor, which can be determined from Table 12.2-1 and Section 11.5.1 of ASCE/SEI 7-10, respectively. Vertically distribute the seismic base shear, V , over the modified building and then perform the elastic static analysis on this building. With the floor displacements resulting from this static analysis, compute the value of A_x (Eq. (4)) for every floor. Following this, vertically distribute V over the twice-modified building, whose eccentricity ratio is $(i-1) \times 0.01 \pm 0.05 A_x$. Perform the elastic static analysis on this twice-modified building. Multiply the peak values of the displacements on all floors resulting from this static analysis with factor C_d/I_e (Eq. (1)) to produce $(EDP_{\pm 0.05 A_x})_{static}$.

Step 4: Compute the DC' value (Eq. (5b)) for every floor by using $(EDP_{\pm 0.05})_{dynamic}$ and $(EDP_{\pm 0.05 A_x})_{static}$ obtained at Steps 2 and 3, respectively. The maximum of the absolute DC' values among all floors is the j -th outcome of the random variable $|DC'|$.

Step 5: Set $j=j+1$. If $j \leq NM$, then go to Step 2.

Step 6: With the NM outcomes of the random variable $|DC'|$ thus far, compute the lognormal cumulative distribution function (CDF) of the random variable $|DC'|$. This CDF is denoted by $G_{dc'}(e)$, where e is the existing eccentricity ratio equal to $(i-1) \times 0.01$. Before computing the aforementioned lognormal CDF, the goodness-of-fit test, e.g., the Kolmogorov–Smirnov test (Ang and Tang 2007), should be performed to ensure that the NM outcomes form a lognormal distribution.

Step 7: Compute the exceedance probabilities, $P[|DC'| \geq dc' | e] = 1 - G_{dc'}(e)$, corresponding to the four discrepancy states of the random variable $|DC'|$ (Table 3). The values of the four exceedance probabilities are denoted by $P_{dc'1}(e)$, $P_{dc'2}(e)$, $P_{dc'3}(e)$, and $P_{dc'4}(e)$.

Step 8: Set $i=i+1$ and $j=1$. If $i \leq NE$, then go to Step 2.

Step 9: There are a total of NE exceedance probabilities for each discrepancy state that corresponds to the NE existing eccentricity ratios, at this stage. For example, there are $P_{dc'1}(0)$, $P_{dc'1}(0.01)$, $P_{dc'1}(0.02)$, ..., $P_{dc'1}(0.3)$ for the discrepancy state $dc'1$. By using the nonlinear least-

square-error method, find the lognormal CDF for the best fit of these NE exceedance probabilities belonging to the same discrepancy state. The curve of this lognormal CDF is the discrepancy curve, which is a function of the existing eccentricity ratio. The four discrepancy curves corresponding to the four discrepancy states are eventually obtained.

In addition to obtaining the exceedance probabilities of the discrepancy states, it is also useful to examine the degree of underestimation or overestimation of seismic responses computed from the elastic static analysis method including the accidental torsion effects. Therefore, the average of DC' values, rather than $|DC'|$ values, for all floors under the excitations of all applied ground motions is also computed for every building. That is, the average DC' value of a building with a

certain existing eccentricity ratio is computed as $\sum_{j=1}^{NM} \sum_{k=1}^{NF} DC' / (NM \times NF)$, where NF is the number of floors.

3. Evaluation results

3.1 Model buildings and selected ground motions

Three types of building, namely 3-story, 9-story, and 20-story steel moment-resisting buildings, were investigated in this study. These 3-story, 9-story, and 20-story model buildings, referred to as SAC3, SAC9, and SAC20, respectively, are variations of the prototype buildings (Fig. 2) used in the SAC steel research project (FEMA-355C 2000) for buildings located in Los Angeles. The prototype buildings were designed according to UBC (1994) provisions, which stipulate the strong-column-weak-beam requirement. The prototype buildings were designed as typical office buildings situated on stiff soil (FEMA-355C 2000). The variations adopted in the current study include CMs of each prototype building that were shifted in the positive z -direction to result in 31 existing eccentricity ratios varying from 0% to 30% in 1% increments. In addition, the floor mass moment of inertia of each prototype building was scaled to result in four different frequency ratios: $\Omega=0.7, 1.0, 1.3,$ and 1.6 . The frequency ratio Ω is the ratio of the frequency of the first rotational mode to the frequency of the first translational mode of the corresponding symmetrical building. The purpose of considering different frequency ratios is to investigate asymmetric-plan buildings with different rotational properties. When the frequency ratio is lower or higher than one, the building is torsionally flexible or torsionally stiff, respectively. When the frequency ratio is approaching one or equal to one, the building is torsionally similarly stiff.

The materials of the beams and columns used in these model buildings were Dual A36 Gr. 50 steel and A572 Gr. 50 steel, respectively. The yield strengths of these two steel materials were 340 and 345 MPa, respectively. The simulated stress-strain relationships of these two steel materials were bilinear with Young's modulus $E=2.0 \times 10^5$ MPa and 3% post-yielding stiffness ratio. All of the beam and column members were represented by using beam-column elements with concentrated plasticity simulated as plastic hinges at the two ends of each element. Rigid diaphragms were assumed for all floors. The P- Δ effects were not included in the static nor in the dynamic analyses. The PISA3D computer program (Lin *et al.* 2009) was used for the numerical analyses.

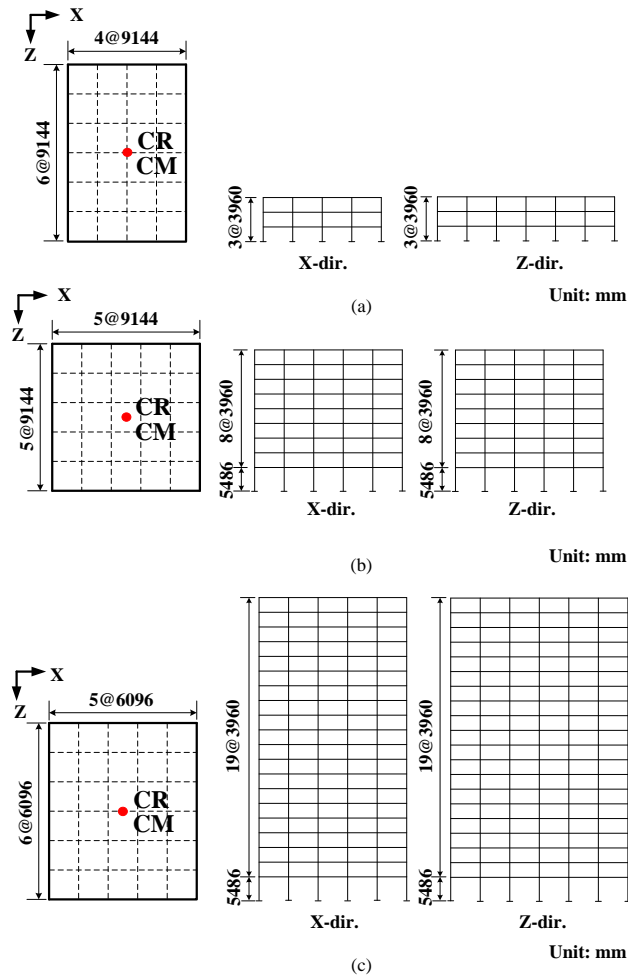


Fig. 2 Typical floor plans and elevations of the (a) 3-story, (b) 9-story, and (c) 20-story prototype buildings

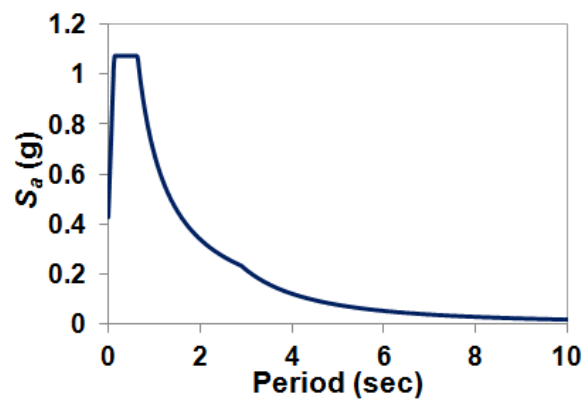


Fig. 3 Design response spectrum

A total of 372 (i.e., $3 \times 4 \times 31$) buildings were analyzed in this study. The importance factor, I_e , was set to equal one for all model buildings. As these 372 model building structures are steel special moment frames, the values of factors C_d and R are 5.5 (Table 1) and 8 (Table 12.2-1 in ASCE/SEI 7-10), respectively. The total weights, W , of the 3-story, 9-story, and 20-story buildings are 30,453 kN, 88,393 kN, and 108,619 kN, respectively (FEMA-355C 2000). The design response spectrum with a 475-year return period used for the prototype buildings located in Los Angeles is shown in Fig. 3, in accordance with the SAC report (FEMA-355C 2000). Using Fig. 3 and the fundamental vibration period of each building, the corresponding seismic base shear, V (Eq. (6)), was computed accordingly.

The selected ground motions were the ensemble of twenty earthquake records used in the SAC project for the hazard level of a 475-year return period in Los Angeles. These twenty ground motions were applied to all model buildings in the x -direction. Rayleigh damping was assigned to all buildings, whereby the damping ratios of the first two x -translational dominant modes of each building were set to 2%. The periods of the first x -directional vibration modes of the 3-story, 9-story, and 20-story prototype buildings are 1.05, 2.28, and 3.85 s, respectively. The details of the twenty selected ground motion records are available in the SAC report (FEMA-355C 2000).

3.2 Average DC' values

Figs. 4 and 5 show the average DC' values for all floors under the excitation of all applied ground motions when the accidental eccentricity ratio is 5% and -5% , respectively. Fig. 4 shows that most of the average displacement estimates at the CM, FS, and SS are overestimated using the elastic static analysis approach. In particular, for the average displacement estimates at the CM and FS, the only underestimated case occurs at the torsionally flexible ($\Omega=0.7$) SAC3, which belongs to the class of low-rise buildings (Figs. 4(a) and 4(b)). For the average displacement estimates at the SS, the un-conservative cases include torsionally flexible ($\Omega=0.7$) SAC3 and torsionally similarly stiff ($\Omega=1.0$) SAC3. Additionally, the average displacement estimates at the SS of SAC3 with $\Omega=1.3$ and SAC9 with $\Omega=0.7$ are also underestimated when their existing eccentricity ratio e is larger than 10% (Fig. 4(c)).

The abovementioned trends shown in Fig. 4 are generally consistent with those presented in Fig. 5, of which the latter corresponds to an accidental eccentricity ratio of -5% . The only exception is when $e > 10\%$, as mentioned in Fig. 4, is modified to $e > 20\%$, as shown in Fig. 5, which underestimates the average DC' values for SAC3 with $\Omega=1.3$ and SAC9 with $\Omega=0.7$. This is because the total eccentricity ratio with the existing eccentricity ratio of 10% plus the accidental eccentricity ratio of 5% is the same as the existing eccentricity ratio of 20% plus the accidental eccentricity ratio of -5% .

Furthermore, Figs. 4 and 5 show that the average DC' values increase as the building height increases. In other words, the errors resulting from the elastic static analysis approach essentially become more critical for taller buildings. The main reason may be that the elastic static analysis approach cannot reflect the effects of the higher modes of taller buildings. Figs. 4 and 5 also show that the average DC' values for the displacements at the CM and FS generally increase as the existing eccentricity ratio increases. Nevertheless, the average DC' values for the displacements at the SS generally decrease as the existing eccentricity ratio increases.

It may be concluded from Figs. 4 and 5 that, by using C_d and A_x , the elastic static analysis approach is effective for estimating the displacements at the CM and FS of torsionally stiff and torsionally similarly stiff low-rise buildings, whose floor plan can vary from symmetric to

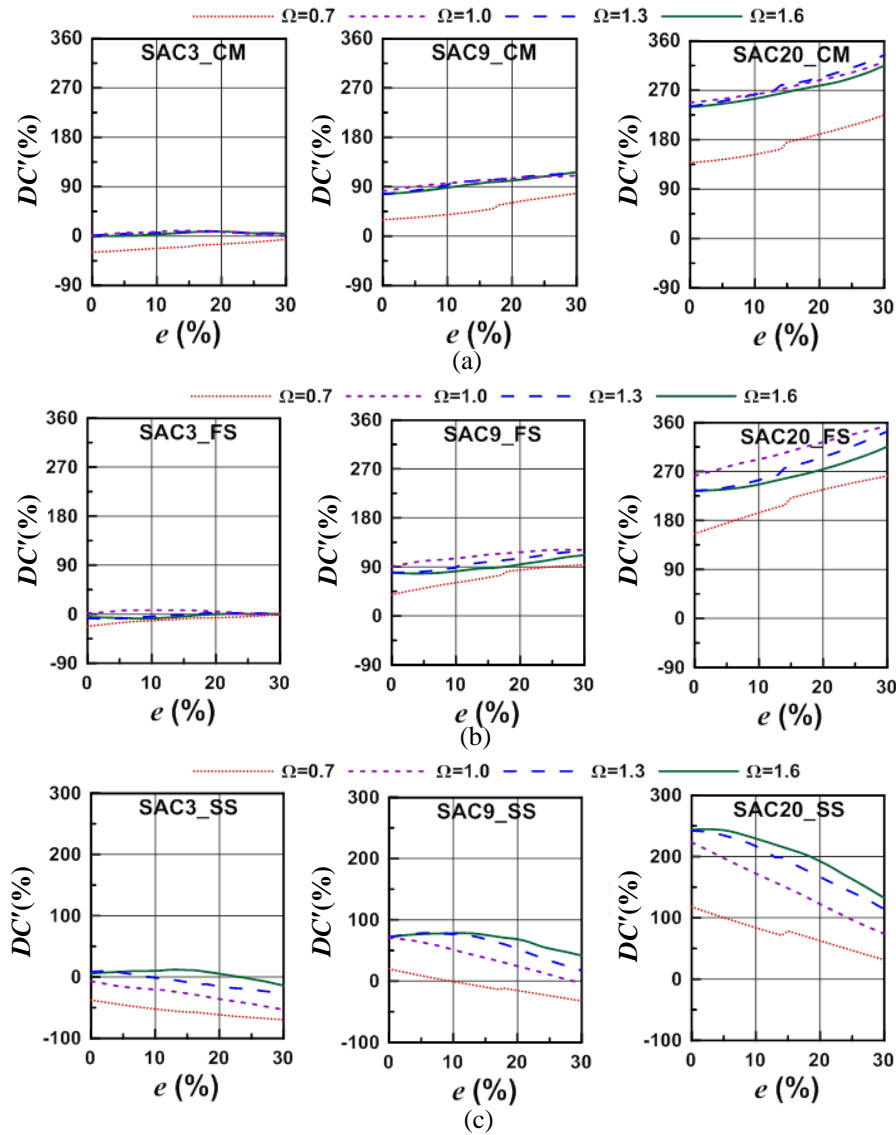


Fig. 4 Average DC' values of displacement estimates at the (a) CM, (b) FS, and (c) SS for SAC3, SAC9, and SAC20 with an accidental eccentricity ratio of 5%

substantially asymmetric. When estimating the displacements at the SS, it is suggested that the elastic static analysis approach is applied only to torsionally stiff low-rise buildings with small existing eccentricity ratios, e.g., less than 10%. For mid-rise and high-rise buildings, the elastic static analysis approach generally results in displacement estimates that are too conservative to be acceptable.

From Figs. 4 and 5, it is noted that the trends of the average DC' values in terms of the frequency ratio are not consistent. For example, when estimating the SS design displacements, the elastic static analysis becomes more conservative as the buildings become more torsionally-stiff

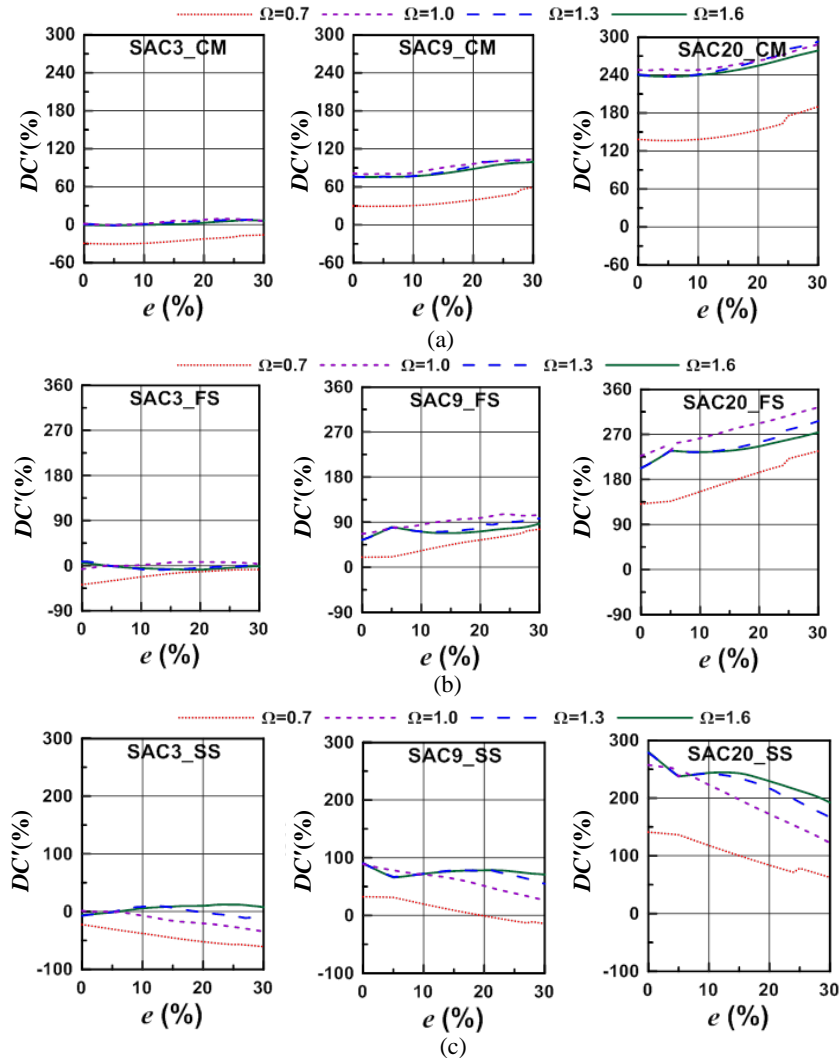


Fig. 5 Average DC' values of displacement estimates at the (a) CM, (b) FS, and (b) SS for SAC3, SAC9, and SAC20 with an accidental eccentricity ratio of -5%

(Figs. 4(c) and 5(c)). Conversely, except the case of $\Omega=0.7$, the elastic static analysis becomes less conservative for estimating the design displacements on the FS (Figs. 4(b) and 5(b)) and CM (Figs. 4(a) and 5(a)) as the buildings become more torsionally-stiff. By defining the torsional effect as the ratio of the displacement on the floor edge to that at the CM, Fajfar *et al.* (2005) pointed out that torsional effects generally decrease when plastic deformations increase. They also mentioned that it is difficult to make general conclusions about the torsional effects on the SS. Lin *et al.* (2012) investigated the reasons behind these torsional effects. Nevertheless, owing to the DC' values are also related to the static analysis results (Eq. (5b)), it becomes more difficult to explain the aforementioned inconsistent trends of the average DC' values in terms of the frequency ratio. These trends appear worth more research.

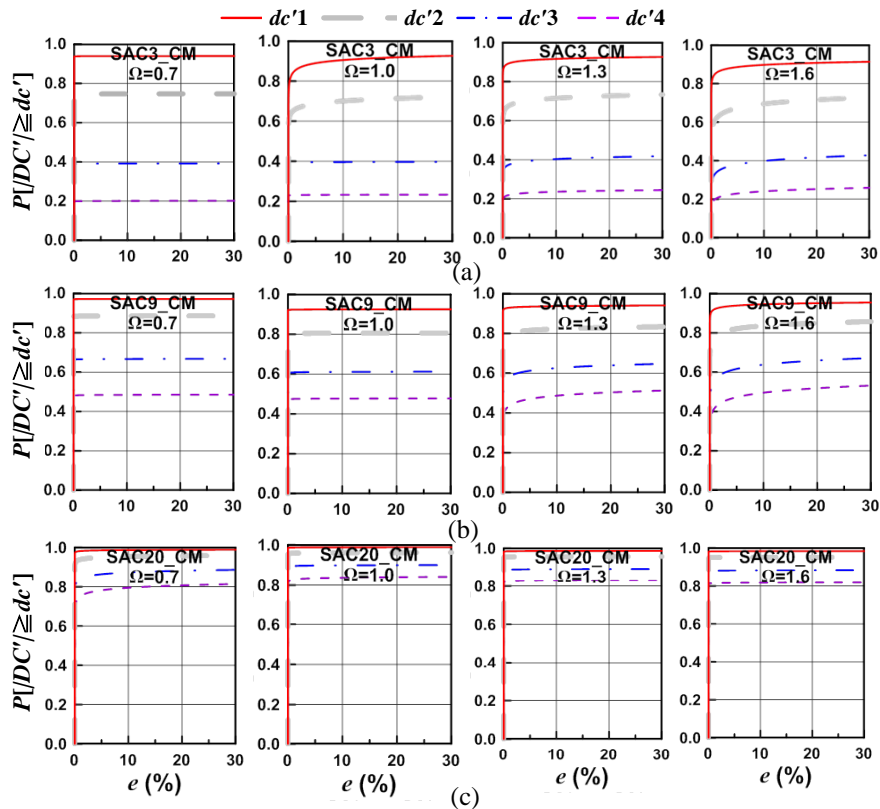


Fig. 6 Discrepancy curves of the statically estimated displacements on the CM of (a) SAC3, (b) SAC9, and (c) SAC20 with an accidental torsion eccentricity ratio of 5%

3.3 Exceedance probabilities of the discrepancy states

Figs. 6(a), 6(b), and 6(c) show the discrepancy curves for the statically estimated displacements at the CM of SAC3, SAC9, and SAC20, respectively, with an accidental torsion eccentricity ratio of 5%. Comparing Figs. 6(a), 6(b), and 6(c) shows that the exceedance probabilities of the discrepancy states increase as the building height increases. In other words, the displacement estimates resulting from the elastic static analysis approach mostly likely deviate from the ‘exact’ displacement responses for SAC20 and least likely for SAC3. This observation is consistent with that obtained from Figs. 4 and 5, in which the average DC' values increase as the building height increases. Figure 6 also indicates that the discrepancy curves for the displacement estimates at the CMs of buildings with the same building height but with different frequency ratios, i.e., $\Omega=0.7$, 1.0, 1.3, and 1.6, are generally the same. The only modest difference is between torsionally flexible buildings ($\Omega=0.7$) and other buildings with frequency ratios of $\Omega=1.0$, 1.3, and 1.6. Therefore, regardless of the difference between frequency ratios, the reliabilities of using the elastic static analysis approach to estimate the design displacements at the CMs of buildings with the same building height are generally the same.

Figs. 7(a), 7(b), and 7(c) show the discrepancy curves for the statically estimated displacements on the FS of SAC3, SAC9, and SAC20, respectively, with an accidental torsion eccentricity ratio

of 5%. The trends shown in Fig. 7 are the same as those discussed for Figs. 6(a), 6(b), and 6(c). Nevertheless, some of the trends shown in the accompanying Figs. 8(a), 8(b), and 8(c), i.e., the discrepancy curves of the displacement estimates on the SS, are different from those on the CM (Fig. 6) and FS (Fig. 7). First, compared with other accompanying figures (Figs. 6, 7, 8(b), and 8(c)), Fig. 8(a) indicates that the exceedance probabilities of the discrepancy states for the estimated displacements on the SS of SAC3 with $\Omega=0.7$ and 1.0 are substantially affected by the existing eccentricity ratio. These exceedance probabilities essentially increase as the existing eccentricity ratio increases. Nevertheless, this property does not obviously exist in other cases shown in Figs. 6 to 8. In other words, the reliability of the displacement estimates resulting from the elastic static analysis approach is not clearly influenced by the existing eccentricity ratio, except when estimating the SS displacements of SAC3 with $\Omega=0.7$ and 1.0. Second, Fig. 8(a) shows that the frequency ratio plays a substantial role in determining the exceedance probabilities of the discrepancy states for the estimated displacements on the SS of SAC3. These exceedance probabilities significantly decrease as the frequency ratio increases. This property does not exist in other cases shown in Figs. 6 to 8. That is to say, the reliability of the displacement estimates resulting from the elastic static analysis approach is not significantly influenced by the frequency ratio except when estimating the SS displacements of SAC3.

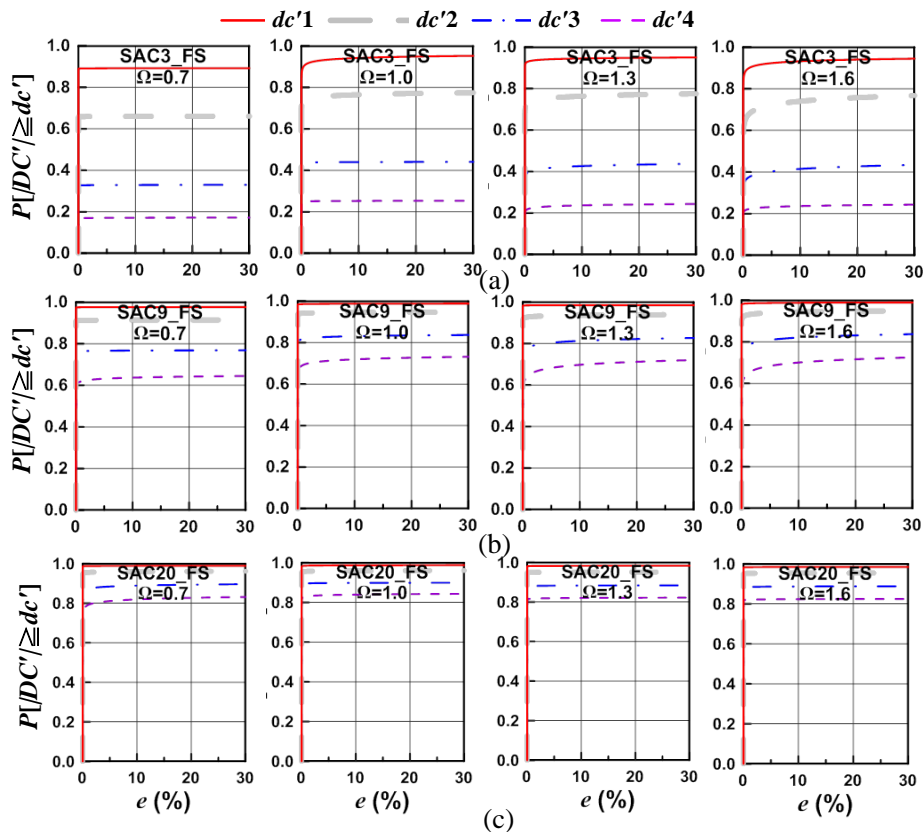


Fig. 7 Discrepancy curves of the statically estimated displacements on the FS of (a) SAC3, (b) SAC9, and (c) SAC20 with an accidental torsion eccentricity ratio of 5%

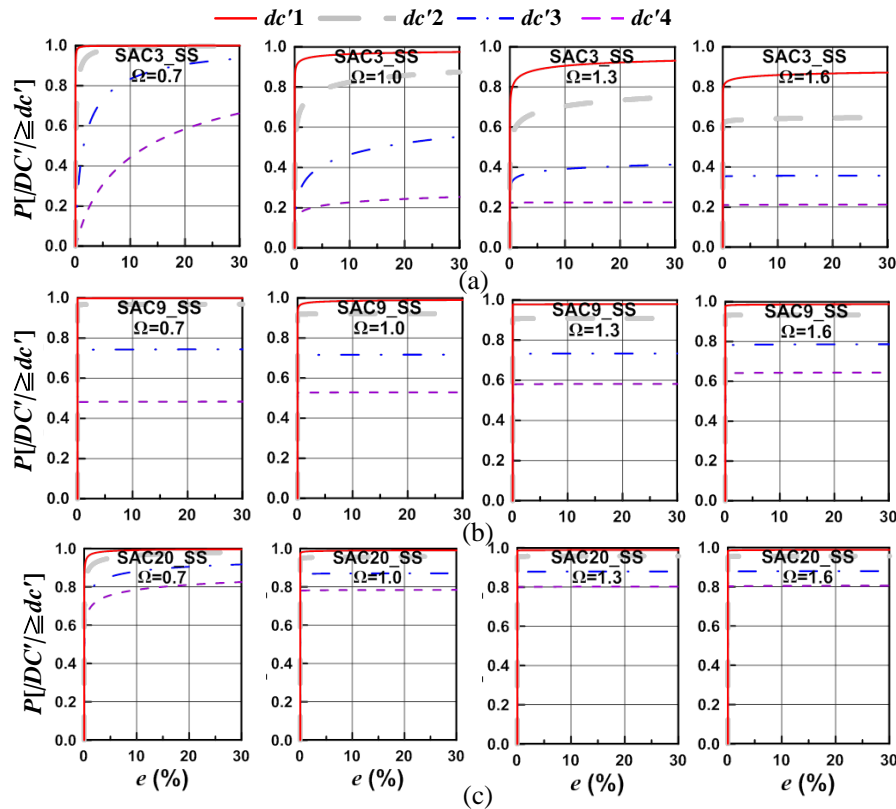


Fig. 8 Discrepancy curves of the statically estimated displacements on the SS of (a) SAC3, (b) SAC9, and (c) SAC20 with an accidental torsion eccentricity ratio of 5%

Table 4 presents the values of the medium, λ , and the logarithmic standard deviation, β , of the discrepancy curves shown in Figs. 6 to 8. By using the values of λ and β given in Table 4, every discrepancy curves, which are lognormal CDFs, can be completely determined. It was found that the properties of the discrepancy curves for the example buildings with a -5% existing eccentricity ratio are the same as those with a 5% existing eccentricity ratio.

Table 5(a) presents the maximum ordinate values of every discrepancy curve shown in Figs. 6 to 8. Thus, the maximum exceedance probability of every discrepancy state for the estimated design displacements on the CM, FS, and SS of the example buildings are available from Table 5a. For example, the maximum exceedance probabilities of discrepancy state $dc'4$ for the displacement estimates at the CM of SAC3, SAC9, and SAC20 are 0.26, 0.53, and 0.84, respectively (Table 5(a)). The probability values were set within the ranges of 0% to 33%, 33% to 66%, and 66% to 100% to represent small (S), medium (M), and large (L) chances, respectively. Consequently, the chance of errors reaching an unacceptable state, i.e., discrepancy values larger than 60%, in estimating the displacements at the CMs of SAC3, SAC9, and SAC20 were small, medium, and large, respectively. Due to the fact that the existing eccentricity ratio and frequency ratio are not clearly influential on the exceedance probabilities of discrepancy states for estimated displacements, except when estimating SS displacements of SAC3, Table 5(a) is further simplified as Table 5(b) for brevity. The average probability shown in Table 5(b) is the average value of the

Table 4 Mean values and standard deviations of discrepancy curves $dc'1$, $dc'2$, $dc'3$, and $dc'4$ for (a) SAC3, (b) SAC9, and (c) SAC20 with an accidental torsion eccentricity ratio of 5%

(a)									
Ω	Location	$dc'1$		$dc'2$		$dc'3$		$dc'4$	
		λ	β	λ	β	λ	β	λ	β
0.7	CM	-628.05	406.47	-487.87	737.00	242.00	873.85	427.57	508.29
	FS	-583.08	472.71	-339.94	829.12	311.47	699.66	361.09	378.01
	SS	-7.13	2.87	-2.62	2.12	0.39	1.98	2.59	1.94
1.0	CM	-8.23	8.04	-7.17	18.04	132.16	491.36	369.31	501.74
	FS	-15.60	11.38	-22.94	34.94	78.30	503.55	290.83	432.88
	SS	-10.51	7.14	-2.38	5.03	2.74	4.91	11.73	12.57
1.3	CM	-20.00	16.18	-8.94	19.80	9.34	28.75	30.63	39.38
	FS	-35.73	23.78	-18.12	28.50	9.37	38.03	38.30	50.25
	SS	-6.27	6.53	-1.98	7.95	7.58	19.15	460.25	605.04
1.6	CM	-12.25	11.51	-3.49	11.38	6.08	14.67	15.70	19.01
	FS	-13.71	10.74	-5.88	12.72	7.08	22.22	37.36	48.83
	SS	-18.06	18.94	-24.18	73.17	178.60	478.13	428.81	533.54
(b)									
Ω	Location	$dc'1$		$dc'2$		$dc'3$		$dc'4$	
		λ	β	λ	β	λ	β	λ	β
0.7	CM	-532.83	281.01	-575.74	480.59	-239.70	561.32	21.23	489.14
	FS	-409.39	208.51	-372.14	274.61	-182.48	253.32	-15.35	50.45
	SS	-76.36	26.10	-217.07	118.37	-337.85	520.00	41.02	915.54
1.0	CM	-378.42	265.13	-302.15	353.85	-91.54	333.46	31.68	507.00
	FS	-129.15	58.81	-123.44	78.65	-41.92	46.18	-14.96	29.73
	SS	-15.79	8.32	-309.30	220.89	-306.13	538.50	-61.89	893.34
1.3	CM	-53.95	36.76	-21.21	25.39	-3.87	19.23	2.85	16.80
	FS	-323.01	151.11	-56.02	38.32	-16.17	20.81	-6.19	16.43
	SS	-410.81	204.58	-483.94	366.64	-400.65	647.98	-177.74	877.38
1.6	CM	-17.83	12.58	-9.67	12.25	-1.98	12.11	2.44	12.13
	FS	-55.96	25.90	-29.86	20.30	-13.06	16.76	-5.65	15.13
	SS	-58.62	27.75	-384.63	257.40	-198.03	253.62	-159.10	439.51
(c)									
Ω	Location	$dc'1$		$dc'2$		$dc'3$		$dc'4$	
		λ	β	λ	β	λ	β	λ	β
0.7	CM	-37.94	18.19	-26.62	17.26	-16.31	16.36	-10.71	15.81
	FS	-290.64	128.80	-90.68	53.16	-32.53	28.52	-18.23	22.52
	SS	-7.34	4.05	-5.39	4.26	-3.94	5.30	-3.57	7.46
1.0	CM	-166.72	74.85	-126.21	72.87	-163.38	130.51	-59.46	63.12
	FS	-102.39	47.21	-126.29	73.75	-247.90	196.93	-65.82	68.73
	SS	-35.68	16.66	-79.74	48.07	-239.25	214.72	-292.11	376.48
1.3	CM	-156.85	72.78	-283.15	166.96	-247.99	203.37	-165.17	176.34
	FS	-228.98	109.30	-281.45	171.59	-244.62	207.60	-162.02	179.21
	SS	-158.66	70.75	-285.27	166.98	-352.47	303.27	-386.75	459.20

Table 4 Continued

1.6	CM	-229.60	109.34	-272.59	166.26	-244.82	208.80	-215.74	240.20
	FS	-229.38	107.49	-282.63	169.33	-246.26	205.82	-217.84	236.99
	SS	-102.39	46.87	-282.85	167.55	-351.40	302.54	-302.46	355.38

Table 5 (a) Maximum exceedance probabilities of every discrepancy curve for the example buildings with an accidental torsion eccentricity ratio of 5%

Ω		CM				FS				SS			
		0.7	1	1.3	1.6	0.7	1	1.3	1.6	0.7	1	1.3	1.6
SAC3	<i>dc'1</i>	0.94	0.93	0.93	0.91	0.89	0.95	0.95	0.94	1.00	0.97	0.93	0.87
	<i>dc'2</i>	0.75	0.72	0.73	0.73	0.66	0.77	0.77	0.77	1.00	0.87	0.75	0.65
	<i>dc'3</i>	0.39	0.40	0.42	0.43	0.33	0.44	0.44	0.43	0.94	0.55	0.41	0.36
	<i>dc'4</i>	0.20	0.23	0.24	0.26	0.17	0.25	0.24	0.24	0.66	0.25	0.23	0.21
SAC9	<i>dc'1</i>	0.97	0.93	0.94	0.95	0.98	0.99	0.98	0.99	1.00	0.99	0.98	0.99
	<i>dc'2</i>	0.89	0.81	0.83	0.86	0.91	0.95	0.94	0.95	0.97	0.92	0.91	0.93
	<i>dc'3</i>	0.67	0.61	0.65	0.67	0.77	0.84	0.83	0.84	0.74	0.72	0.73	0.79
	<i>dc'4</i>	0.49	0.48	0.51	0.53	0.64	0.73	0.72	0.73	0.48	0.53	0.58	0.64
SAC20	<i>dc'1</i>	0.99	0.99	0.99	0.98	0.99	0.99	0.98	0.98	1.00	0.99	0.99	0.99
	<i>dc'2</i>	0.96	0.96	0.96	0.95	0.96	0.96	0.95	0.95	0.98	0.96	0.96	0.96
	<i>dc'3</i>	0.89	0.90	0.89	0.88	0.90	0.90	0.88	0.89	0.92	0.87	0.88	0.88
	<i>dc'4</i>	0.81	0.84	0.83	0.82	0.83	0.84	0.82	0.82	0.82	0.78	0.80	0.81

Table 5 (b) Average probabilities and chance levels in every discrepancy state for the example buildings with an accidental torsion eccentricity ratio of 5%

Bldg.	Discrepancy state	CM		FS		SS	
		Average probability	Chance level	Average probability	Chance level	Average probability	Chance level
SAC3	<i>dc'1</i>	0.93	L	0.93	L	(0.94)	(L)
	<i>dc'2</i>	0.73	L	0.74	L	(0.82)	(L)
	<i>dc'3</i>	0.41	M	0.41	M	(0.57)	(M)
	<i>dc'4</i>	0.23	S	0.23	S	(0.34)	(M)
SAC9	<i>dc'1</i>	0.95	L	0.99	L	0.99	L
	<i>dc'2</i>	0.85	L	0.94	L	0.93	L
	<i>dc'3</i>	0.65	M	0.82	L	0.75	L
	<i>dc'4</i>	0.50	M	0.71	L	0.56	M
SAC20	<i>dc'1</i>	0.99	L	0.99	L	0.99	L
	<i>dc'2</i>	0.96	L	0.96	L	0.97	L
	<i>dc'3</i>	0.89	L	0.89	L	0.89	L
	<i>dc'4</i>	0.83	L	0.83	L	0.80	L

Note:

1. L: large, M: medium, S: small.

2. The numbers in parentheses will change significantly according to the values of the existing eccentricity ratio and frequency ratio of the buildings.

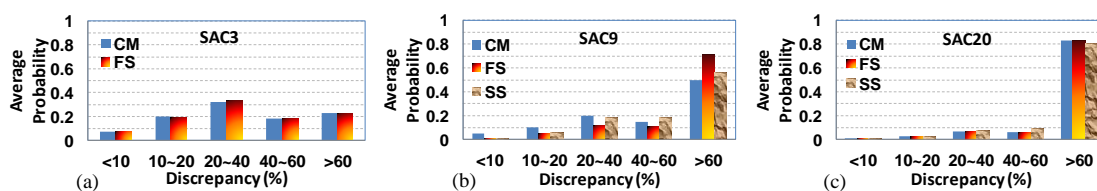


Fig. 9 Average probability distributions of discrepancy for estimated design displacements of (a) SAC3, (b) SAC9, and (c) SAC20

corresponding maximum exceedance probabilities for different frequency ratios ($\Omega=0.7, 1.0, 1.3,$ and 1.6) shown in Table 5(a). Table 5(b) indicates the average probabilities of discrepancy states $dc'1, dc'2, dc'3, dc'4$ for the estimated design displacements at the CM of SAC3 fall into the large (L), large (L), medium (M) and small (S) chance levels, respectively. While for SAC9 and SAC20, these chance levels are L/L/M/M and L/L/L/L, respectively. In addition, the chance levels corresponding to the FS of SAC3 remain L/L/M/S. While for the FS and SS of SAC9 and SAC20, the chance levels almost all fall into the large level (L). Therefore, instead of looking into every curve of Figs. 6 to 8, Table 5(b) gives an effective snap shot of the reliability of using the elastic static method to estimate the design displacements for SAC3, SAC9 and SAC20.

Furthermore, by using the data presented in Table 5(b), the average probabilities for a discrepancy of less than 10%; between 10% and 20%; between 20% and 40%; between 40% and 60%; and larger than 60% are available as shown in Fig. 9. For instance, the discrepancy for the estimated displacements on the CM of SAC3 less than 10%; between 10% and 20%; between 20% and 40%; between 40% and 60%; and larger than 60% are 0.07 (i.e., $1-0.93$); 0.2 (i.e., $0.93-0.73$); 0.32 (i.e., $0.73-0.41$); 0.18 (i.e., $0.41-0.23$); and 0.23, respectively. That is, Fig. 9 illustrates the average probability distributions of the discrepancy on the estimated design displacements of SAC3, SAC9, and SAC20. Although Table 5(b) and Fig. 9 are inducible from Table 5(a), both Table 5(b) and Fig. 9 summarize and present the analysis results (Figs. 6 to 8, and Table 5(a)) in different forms. Using Table 5(b) and Fig. 9 may be helpful for the comprehension of the overall analysis results from different aspects.

4. Conclusions

Instead of nonlinear response history analysis (NRHA), the code-specified elastic static analysis approach is widely used owing to its simplicity in estimating the design displacements of buildings. Furthermore, considering the influence of accidental torsion on the design displacements is mandated whether the buildings are symmetric-plan or asymmetric-plan. This study thoroughly assessed the reliability of statically estimated design displacements by examining the average discrepancy values and the exceedance probabilities of discrepancy states. The discrepancy, denoted by DC' , was defined as the normalized difference between the design displacements resulting from the elastic static analysis approach and from NRHA results. The conclusions and suggestions of this study are as follows:

1. The discrepancy curves for the estimated design displacements on the SSs of low-rise buildings are clearly affected by the values of the existing eccentricity ratio and frequency ratio. As the existing eccentricity ratio increases or the frequency ratio decreases, the corresponding exceedance probabilities of discrepancy states increase (Fig. 8(a)). Nevertheless,

the effect of the existing eccentricity ratio and frequency ratio on other cases is not as apparent when compared with the estimated SS design displacements of low-rise buildings.

2. For low-rise buildings, the code-specified elastic static analysis approach reliably estimates the design displacements at the CM and FS of torsionally stiff and torsionally similarly stiff buildings with $0 \leq e \leq 30\%$. The corresponding exceedance probability of discrepancy state $dc'3$ (i.e., $|DC'|=40\%$) is approximately 41% (Table 5b). Nevertheless, when applying the same approach to estimate the design displacements on the SS of low-rise buildings, the only suitable type of building is torsionally stiff with a small existing eccentricity ratio, i.e., $e \leq 10\%$ (Fig. 4(c)). The corresponding exceedance probability of discrepancy state $dc'3$ is approximately 40% (Fig. 8(a)).

3. For mid-rise and high-rise buildings, the code-specified elastic static analysis approach significantly overestimates the design displacements. The exceedance probabilities of discrepancy state $dc'4$ (i.e., $|DC'|=60\%$) for mid-rise and high-rise buildings are approximately 50% and 80%, respectively (Table 5(b)). For the large chance of resulting in a high discrepancy ($dc'4$), the code-specified elastic static analysis approach appears to be inappropriate for estimating the design displacements of mid-rise and high-rise buildings.

The building structures investigated in this study consisted of steel special moment frames. The reliabilities of estimated design displacements for other types of building systems are worth exploring in future research.

References

- Ang, A.H.S and Tang, W.H. (2007), *Probability concepts in engineering: emphasis on applications to civil and environmental engineering*, 2nd Edition, Wiley.
- ASCE (2010), *Minimum Design Loads for Buildings and other Structures*. ASCE/SEI 7–10. American society of Civil Engineers (ASCE): Reston, VA.
- Chopra, A.K. and Chintanapakdee, C. (2004), “Inelastic deformation ratios for design and evaluation of structures: single-degree-of-freedom bilinear systems”, *J. Struct. Eng.*, ASCE, **130**(9), 1309-1319.
- DeBock, D.J., Liel, A.B., Haselton, C.B., Hoopper, J.D. and Henige, Jr. R.A. (2013), “Importance of seismic design accidental torsion requirements for building collapse capacity”, *Earthq. Eng. Struct. D.*, **43**(6), 831-850.
- De la Llera, J.C. and Chopra, A.K. (1994), “Evaluation of code accidental-torsion provisions from building records”, *J. Struct. Eng.*, ASCE, **120**(2), 597-616.
- De la Llera, J.C. and Chopra, A.K. (1995), “Estimation of accidental torsion effects for seismic design of buildings”, *J. Struct. Eng.*, ASCE, **121**(1), 102-114.
- Dimova, S.L. and Alashki, I. (2003), “Seismic design of symmetric structures for accidental torsion”, *Bul. Earthq. Eng.*, **1**, 303-320.
- Eurocode 8 (2004), *Design of Structures for Earthquake Resistance. Part1: General Rules, Seismic Actions and Rules for Buildings*. prEN 1998-1:2004(E), Commission of the European Communities, European Committee for Standardization, Brussels.
- Fajfar, P. (2000), “A nonlinear analysis method for performance-based seismic design”, *Earthq. Spectra*, **16**(3), 573-592.
- Fajfar, P., Kilar, V., Marusic, D. and Perus, I. (2005), “Torsional effects in the pushover-based seismic analysis of buildings”, *J. Earthq. Eng.*, **9**, 831-854.
- FEMA-355C (2000), *State of the art report on systems performance of steel moment frames subject to earthquake ground shaking*, prepared by the SAC Joint Venture for the Federal Emergency Management Agency, Washington, DC.

- Gupta, B. and Kunnath, S.K. (2000), "Adaptive spectra-based pushover procedure for seismic evaluation of structures", *Earthq. Spectra*, **16**(2), 367-392.
- Humar, J. and Kumar, P. (2000), "A new look at the torsion design provisions in seismic building codes", *Proceedings of the 12th World Conference on Earthquake Engineering, Paper No. 1707*, New Zealand Society for Earthquake Engineering, Upper Hut, New Zealand.
- Iwan, W.D. (1980), "Estimating inelastic response spectra from elastic spectra", *Earthq. Eng. Struct. D.*, **8**, 375-388.
- Kim, S. and D'Amore, E. (1999), "Pushover analysis procedure in earthquake engineering", *Earthq. Spectra*, **15**(3), 417-434.
- Krawinkler, H., Lignos, D.G. and Putman, C. (2011), "Prediction of nonlinear response-pushover analysis versus simplified nonlinear response history analysis", *Structural Congress*, 2228-2239, doi: 10.1061/41171(401)193.
- Krawinkler, H. and Seneviratna, G.D.P.K. (1998), "Pros and cons of a pushover analysis of seismic performance evaluation", *Eng. Struct.*, **20**, 452-464.
- Lin, B.Z., Chuang, M.C. and Tsai, K.C. (2009), "Object-oriented development and application of a nonlinear structural analysis framework", *Adv. Eng. Softw.*, **40**, 66-82.
- Lin, J.L., Tsai, K.C. and Chuang, M.C. (2012), "Understanding the trends in torsional effects in asymmetric-plan buildings", *Bul. Earthq. Eng.*, **10**, 955-965.
- Miranda, E. (2000), "Inelastic displacement ratios for structures on firm sites", *J. Struct. Eng.*, ASCE, **126**(10), 1150-1159.
- Miranda, E. and Ruiz-Garcia, J. (2002), "Evaluation of approximate methods to estimate maximum inelastic displacement demands", *Earthq. Eng. Struct. D.*, **31**, 539-560.
- Ruiz-Garcia, J. and Miranda, E. (2006), "Inelastic displacement ratios for evaluation of structures built on soft soil sites", *Earthq. Eng. Struct. D.*, **35**, 679-694.
- UBC (1994), "Structural Engineering Design Provisions", *Uniform Building Code*, Vol. 2, International Conference of Building Officials.
- UBC (1997), "Structural Engineering Design Provisions", *Uniform Building Code*, Vol. 2, International Conference of Building Officials.
- Veletsos, A.S. and Newmark, N.M. (1960), "Effect of inelastic behavior on the response of simple systems to earthquake motions", *Proceedings of the 2nd World Conf. on Earthquake Engineering*, Vol. II, Tokyo, 895-912.
- Wang, W.C., Lin, J.L. and Tsai, K.C. (2014), Reliability assessment of the torsional amplification factor for accidental torsional moment of buildings subjected to earthquakes. *Report No. NCREE-14-013*, National Center for Research on Earthquake Engineering, Taipei, Taiwan. (in Chinese)